0022-3565/04/3112-492–501$20.00
THE JOURNAL OF PHARMACOLOGY AND EXPERIMENTAL THERAPEUTICS
JPET 311:492–501, 2004

Vol. 311, No. 2
69229/1172684
Printed in U.S.A.

The Preparation and Characterization of Novel Peptide Antagonists to Thrombin and Factor VIIa and Activation of Protease-Activated Receptor 1

Marvin T. Nieman, Mark Warnock, Ahmed A. K. Hasan, Fakhri Mahdi, Benedict R. Lucchesi, Nancy J. Brown, Laine J. Murphey, and Alvin H. Schmaier

Thromgen, Inc., Ann Arbor, Michigan (M.T.N., M.W., A.A.K.H., A.H.S.); Division of Hematology and Oncology, Departments of Internal Medicine (M.T.N., M.W., F.M., A.H.S.) and Pharmacology (B.R.L.), University of Michigan Medical School, Ann Arbor, Michigan; and Division of Clinical Pharmacology, Departments of Medicine and Pharmacology, Vanderbilt University, Nashville, Tennessee (N.J.B., L.J.M.)

Received March 30, 2004; accepted June 21, 2004

ABSTRACT

Thrombin and protease-activated receptor 1 (PAR1) activation antagonists were prepared based upon the peptide RPPGF, the angiotensin-converting enzyme breakdown product of bradykinin. A library of 72 peptides consisting of D and/or synthetic amino acids was designed with various substitutions in positions 1 to 5 in Arg-Pro-Pro-Gly-Phe (RPPGF). Two compounds, rOicPGF (TH146) and βAK2K-4(rOicPGF) (MAP4-TH146), were characterized further. TH146 or MAP4-TH146 completely inhibits its threshold γ-thrombin-induced platelet aggregation at a concentration of 142 ± 0.05 or 19 ± 0.06 μM, respectively. TH146 completely inhibits threshold α-thrombin-induced washed platelet aggregation at 444 ± 0.04 μM. TH146 or MAP4-TH146 blocks 2 nM α-thrombin-induced fibroblast calcium mobilization with an IC_{50} value of 110 or 18 μM, respectively. Furthermore, significant prolongation of the activated partial thromboplastin time, prothrombin time, or thrombin clotting time occurs at 31, 62, or 7.8 μM TH146 and 0.4, 6.25, or 1.56 μM MAP4-TH146, respectively. TH146 and MAP4-TH146 inhibit both α-thrombin with a K_i value of 97 and 49 μM, respectively, and factor VIIa with a K_i value of 44 and 5 μM, respectively. Both TH146 and MAP4-TH146 specifically bind to the exodomain of recombinant PAR1. MAP4-TH146 (200 μM) completely blocks thrombocytin, a PAR1-activating snake venom protease, without inhibiting the enzyme's active site. TH146 inhibits γ-thrombin-induced aggregation of mouse platelets, prolongs mouse bleeding times, and delays the time to mouse carotid artery thrombosis. TH146 and MAP4-TH146 inhibit human and mouse platelet aggregation and mouse thrombosis. Analogs of RPPGF are model compounds to develop PAR1 activation antagonists as well as direct inhibitors to thrombin and factor VIIa.

Investigations from a number of laboratories indicate that platelet receptors for thrombin are antiplatelet targets. Hanson and Harker (1988) showed that treatment of baboons with Phe-Pro-Arg-chloromethylketone, a potent direct acting thrombin inhibitor, prolongs the bleeding time. More recently, knockout mice of protease-activated receptor (PAR) 3 or 4, mouse platelet thrombin receptors, independently prolong bleeding times and are protected against ferric chloride-induced thrombosis (Weiss et al., 2002). Cook et al. (1995) showed that an IgG raised to a peptide of the hirudin-anionic binding region on the exosite of human PAR1 reduces or abolishes cyclic flow variations in the carotid artery of monkeys. A nonpeptide mimetic (RWJ-58259) directed to the cleaved PAR1 activation site after a 3 mg/kg intravenous bolus followed by a constant infusion of 0.123 mg/kg/min significantly prolongs the time to carotid artery thrombosis in monkeys (Derian et al., 2003). Furthermore, another nonpeptide mimetic at 1 mg/kg directed to the SFLLRN activation site on PAR1 delays the time to guinea pig carotid artery thrombosis (Kato et al., 2003). These combined studies indicate that inhibition of thrombin, thrombin binding to PAR1, and/or PAR1 activation prolongs the bleeding time and delays the time to thrombosis in various animal models.

The plasma protein high molecular weight kininogen

This work was supported by Grant #1607 from the Michigan Economic Development Corporation and National Institutes of Health Grant HL61981 (to A.H.S.), HL04445 (to L.J.M.), and HL65193 (to N.J.B).
Article, publication date, and citation information can be found at http://jpet.aspetjournals.org.
doi:10.1124/jpet.104.069229.

ABBREVIATIONS: PAR, protease-activated receptor; RPPGF, Arg-Pro-Pro-Gly-Phe; TH146, rOicPGF; MAP4-TH146, βAK2K4(rOicPGF); PRP, platelet-rich plasma; APTT, activated partial thromboplastin time; PT, prothrombin time; TCT, thrombin clotting time; FX, factor X; RWJ-58259, (α*S*)-*N*-[(1*S*)-3-amino-1-[[(phenylmethyl)amino]carbonyl]propyl]-α-[[[[1-(2,6-dichlorophenyl)methyl]-3-(1-pyrrolidinylmethyl)-1*H*-indazol-6-yl]amino]carbonyl]amino]-3,4-difluorobenzenepropanamide.

blocks thrombin-induced platelet activation (Meloni and Schmaier, 1991; Puri et al., 1991). The thrombin inhibitory region on kininogen is contained within the angiotensin-converting enzyme breakdown product of bradykinin, Arg-Pro-Pro-Gly-Phe (RPPGF) (Hasan et al., 1996). RPPGF inhibits thrombin-induced platelet activation but not that induced by ADP, collagen, or U46619 (Hasan et al., 1996). It inhibits thrombin-induced platelet aggregation two ways. RPPGF is a weak direct thrombin inhibitor ($K_i = 1.75 \pm 0.03$ mM) with its amino terminal arginine interacting with H^{57}, D^{189}, and S^{195} and its prolines interacting with W^{60d} and W^{215} on thrombin (Hasan et al., 2003). RPPGF also binds to $LDPR^{41}$ and $PRSF^{43}$ on PAR1 with a K_d value of 20 μM to prevent thrombin cleavage at this site and PAR1 activation (Hasan et al., 2003). RPPGF infusion delays the time to occlusion in a canine model of the electrolytically injured coronary artery similar to that of aspirin (Hasan et al., 1999). Furthermore, a multiantigenic peptide form of RPPGF (MAP4-RPPGF) reduced canine coronary artery cyclic flow variations similar to aspirin or clopidogrel (Hasan et al., 2001a). MAP4-RPPGF also reduces platelet adhesion and activation of balloon-injured canine coronary arteries ex vivo like aspirin (Prieto et al., 2002). These combined studies indicate that RPPGF is a novel thrombin inhibitor. The present investigations report the preparation and characterization of modified forms of RPPGF, referred to as Thrombostatin, consisting of peptides containing various D- and synthetic amino acid substitutions.

Materials and Methods

Peptides and Reagents. The abbreviations used for synthetic amino acids are (2*S*,3*aS*,7*aS*)-octahydroindol-2-carboxilic acid (Oic), 4-hydroxyproline (Hyp), α-(2-indanyl)glycine (Idg), and β-(2-thienyl)-L-alanine (Thi). Standard single-letter abbreviations are used for L-amino acids and lowercase letters are used to designate D-amino acids. Peptides RPPGF, scrambled RPPGF, FPRPG, D-Arg-Oic-Pro-Gly-Phe (rOicPGF, TH146, or D-argininyl, octahydroindole-2-carboxylic acid, prolinyl, glycyl, phenylalanine), scrambled TH146 (FOicrPG), D-Arg-Oic-Pro-Gly-Idg (rOicPGIdg or TH34), D-Arg-Oic-Hyp-Gly-Thi (rOicHypGThi or TH37), D-Arg-Oic-Hyp-Gly-Idg (rOicHypGIdg or TH40), D-Arg-Oic-Pro-Gly-Thi (rOicPGThi or TH26), D-Arg-Oic-Oic-Gly-Idg (rOicOicGIdg or TH46), D-Arg-Oic-Oic-Gly-Thi (rOicOicGThi or TH43), and a four branched, multiple antigenic peptide of β-Ala-Lys-2Lys-4(D-Arg-Oic-Pro-Gly-Phe) [[β-A-K-2K-4(rOicPGF)] (MAP4-rOicPGF, MAP4-TH146), or β-alaninyl, lysyl, 2 lysyl, 4 D-argininyl, octahydroindole-2-carboxylic acid, prolinyl, glycyl, phenylalanine] were synthesized by Multiple Peptide Systems, Inc. (San Diego, CA) (Table 1). For MAP4-rOicPGF, β-alanine was attached to a resin core by its carboxyl group followed by the attachment of a lysine via its carboxyl group to the free amine group on the β-alanine. Two additional lysines were attached via their free carboxyl group to the two free amine groups of the first lysine residue. Finally, four rOicPGF peptides were attached via the carboxyl groups of the phenylalanines to each of the four available free amine groups of the two lysine residues after activation with 2-(1-*H*-benzotriazole-1-yl)-1,1,3,3-tetramethyluroniumhexo-fluorophosphate and 1-hydroxybenzotriazole. The final structure of MAP4-TH146 is shown in Structure 1. All peptides used in these studies were >95% pure by reverse-phase high-performance liquid chromatography. The purified peptides were characterized by analytical high-performance liquid chromatography, amino acid analysis, and mass spectrometry for homogeneity. The peptides were colorless, odorless, and soluble in water. D-Arg-Arg-Pro-Hyp-Gly-Thi-Ser-D-Tic-Oic-Arg (HOE140), a bradykinin B2 receptor antagonist, was generously provided by Hoechst Aktiengesellschaft (Frankfurt, Germany).

Platelet Aggregation. Each peptide initially was assayed for its ability to inhibit γ-thrombin-induced platelet aggregation. Fresh whole blood was collected from normal human donors directly into 3.8% sodium citrate (1:9, citrate/blood). Platelet-rich plasma (PRP) was prepared by centrifugation of whole blood at 180*g* (Beckman GRP centrifuge, Schaumburg, IL) for 10 min at room temperature as reported previously (Hasan et al., 1996). Platelet-poor plasma was prepared by centrifugation of the sample of PRP at 1000*g* for 20 min at room temperature. Before all platelet aggregation studies, the platelet count of the PRP was determined on a Coulter counter (model Z; Coulter Electronics, Hialeah, FL) and adjusted to 2.2 to 2.5×10^8 platelets/ml. When mouse platelets were studied, a pool of PRP from 10 mice was prepared in an identical manner as described above for human platelet aggregation studies. Platelet aggregation was assayed by a Chronolog dual-channel aggregometer (Havertown, PA) by recording the increase in light transmittance through a stirred suspension of PRP maintained at 37°C in the cuvette. PRP was treated with variable concentrations of γ-thrombin (3000 U/mg; Hematologic Technologies, Essex Junction, VT) to determine the threshold concentration for platelet aggregation. γ-Thrombin was used for these studies because screening platelet aggregation studies were performed in PRP and γ-thrombin, unlike α-thrombin, will not clot fibrinogen. Platelet aggregation was measured in arbitrary units as the initial rate of change in light transmittance in the first minute after the addition of γ-thrombin; samples were standardized between platelet-poor plasma (100%) and PRP (0%). The effect of each peptide on platelet aggregation was assayed by adding peptides at various concentrations to the cuvette, allowing the baseline to stabilize, and then adding threshold amounts of γ-thrombin (10–70 nM for human platelets, 250–500 nM for mouse platelets). The aggregation was allowed to proceed for 5 min. The minimal concentration of each

TABLE 1

Influence of RPPGF derivatives on γ -thrombin-induced platelet aggregation and calcium mobilization

Data presented are the mean ± S.E.M. of $n > 3$ independent experiments. In all instances, the values given represent the concentration of peptide needed to inhibit threshold γ -thrombin-induced platelet aggregation 100%. Calcium mobilization assays were performed as described under *Materials and Methods*. In all instances, the values given represent the influence of 100 mM peptide on threshold α-thrombin-induced calcium mobilization.

Peptide	Sequence	Platelet Aggregation 100% Inhibitory Conc.	Calcium Mobilization
		mM ± S.E.M.	*Percentage of inhibition at 100 mM peptide*
RPPGF[a]	RPPGF	0.68 ± 0.28	
TH146	ROicPGF	0.142 ± 0.02	54
MAP4-TH146[b]		0.019 ± 0.006	80
TH34	ROicPGIdg	0.129 ± 0.02	36.2
TH37	RoicHypGThi	0.157 ± 0.02	38
TH40	ROicHypGIdg	0.157 ± 0.02	36.7
TH26	ROicPGThi	0.228 ± 0.02	14.5
TH46	ROicOicGIdg	0.257 ± 0.04	28.1
TH43	ROicOicGThi	0.271 ± 0.04	18.1

[a] From Hasan et al. (2001a).
[b] MAP4-TH146 is a multiantigenic peptide of TH146 consisting of β-AK2K-4(rOicPGF).

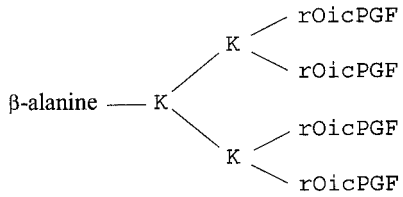

Structure 1.

peptide to achieve full inhibition of platelet aggregation was determined. Platelet aggregation data were expressed as percentage of inhibition of the extent of chart deflection of a peptide-treated platelet sample compared with an untreated sample × 100.

In other experiments, the ability of TH146 to inhibit threshold α-thrombin-induced washed platelet aggregation was determined. Human α-thrombin (3000 U/ml), the physiological form of thrombin, was purchased from Hematologic Technologies. Human platelets in PRP were separated from plasma by gel filtration over Sepharose 2B columns in HEPES-carbonate buffer (137 mM NaCl, 3 mM KCl, 12 mM $NaHCO_3$, 14.7 mM HEPES, 5.5 mM dextrose containing 0.2% bovine serum albumin, pH 7.4) (Hasan et al., 1996). The peak tubes were pooled and the platelet count was adjusted to 2.25×10^8 platelets/ml before proceeding with platelet aggregation studies. When the platelet aggregation was performed, the platelet suspension was made 200 μg/ml with human fibrinogen (Kabi, Stockholm, Sweden) before the addition of the agonist. The aggregation studies were performed as described above. For each platelet donor, the threshold α-thrombin concentration was obtained that initiated full platelet aggregation. Usually, the threshold of α-thrombin-induced platelet aggregation was 1 to 2 nM (0.125–0.25 U/ml).

Calcium Mobilization. Each peptide was assayed for its ability to inhibit α-thrombin-induced calcium mobilization in fibroblasts. Normal human lung fibroblasts were purchased from Clonetics (San Diego, CA) and were cultured according to supplier's instructions. The cytoplasmic free calcium concentration was determined with the Ca^{2+} indicator Fura-2 (Molecular Probes, Eugene, OR). Suspensions of fibroblasts in HEPES-carbonate buffer alone or supplemented with 100 mM Ca^{2+} and Mg^{2+} were loaded with Fura-2 by incubation at 37°C with 5 μM Fura-2/acetoxymethyl ester for 60 min as reported previously (Fisher et al., 1989; Hasan et al., 1996). Excess probe was removed by washing the cells three times. Aliquots of the labeled cells were transferred to a quartz cuvette that was placed in a thermostatically controlled chamber at 37°C in a fluorescence spectrophotometer (LS50B spectrofluorometer; PerkinElmer Life and Analytical Sciences, Boston, MA). Cells were treated with 0.25 to 4.0 nM of α-thrombin (3000–3250 U/mg stock concentration; Hematologic Technologies) to determine the minimal amount needed to produce the maximal response. The concentration of α-thrombin necessary to stimulate intracellular Ca^{2+} mobilization varied 1 order of magnitude, depending upon the presence or absence of extracellular Ca^{2+} and Mg^{2+}. The effect of each peptide was determined by adding variable concentrations of peptide to the cells followed by threshold levels of α-thrombin and readings taken as described below. The excitation wavelengths varied between 340 and 380 nm, and fluorescence was measured by recording light emitted at 510 nm as described by Fisher et al. (1989). The degree of inhibition of α-thrombin induced Ca^{2+} flux for each peptide was determined by calculating the area under the curve by Winlab software (PerkinElmer Life and Analytical Sciences) and is expressed as percentage of activity; samples without peptide (thrombin alone) were set to 100%.

Clotting Assays. The effect of TH146 or MAP4-TH146 on the activated partial thromboplastin time (APTT), prothrombin time (PT), and thrombin clotting time (TCT) was determined. APTT and PT were performed as described previously in the presence or absence of increasing concentrations of peptide (Hasan et al., 1999, 2001a, 2003). Thrombin clotting time was determined by incubating 100 μl of pooled normal human plasma (George King, Inc., Overland Park, KS) in the absence or presence of peptide at 37°C for 5 min. At the end of the incubation, 8 nM human α-thrombin (Hematological Technologies) was added and the time to clot was measured. All the coagulant assays were performed in Amelung KC4 coagulation analyzer (Sigma-Aldrich, St. Louis, MO). Values were considered significantly prolonged when the mean result at each concentration of the inhibitor was $p < 0.05$ from the control on a nonpaired t test.

Enzymatic Assays. The ability of 142 μM TH146 and 200 μM MAP4-TH146 to inhibit the hydrolytic activity of human α-thrombin (1 nM) or γ-thrombin (1 nM) was measured in 10 mM Tris-HCl, 0.15 M NaCl, pH 7.6, containing 0.1% bovine serum albumin, using 0.6 mM Sar-Pro-Arg-paranitroanilide (Sigma-Aldrich) (K_m = 138 μM) (Hasan et al., 2003). Additional studies determined the ability of these compounds to inhibit 3 nM factor XIa (FXIa) (Hematologic Technologies) in the same buffer hydrolysis of 0.6 mM L-pyro-Glu-Pro-Arg-paranitroanilide (Diaphram, Franklin, OH) (Hasan et al., 2001a). Inhibition of 1 nM factor Xa (FXa) (Enzyme Research Laboratories Inc., South Bend, IN) in 100 mM triethanolamine, 100 mM NaCl, pH 8.0, supplemented with 0.1% polyethyleneglycol (mol. wt. 8000) and 0.2% bovine serum albumin was determined using 0.4 mM *N*-(*p*-Tosyl)-Gly-Pro-Arg-paranitroanilide (Schmaier et al., 1995). Inhibition of 50 nM factor VIIa (FVIIa) (Hematologic Technologies) in a preformed complex with 70 nM soluble recombinant tissue factor, amino acids 1–219 (sTF_{1-219}), provided by Dr. Tom Girard (Monsanto, St. Louis, MO) in 0.02 M Tris-HCl, 0.14 M NaCl, pH 7.4, containing 0.1% bovine serum albumin and 5 mM $CaCl_2$ was determined by hydrolysis of 1.25 mM methoxycarbonyl-D-cyclohexylglycyl-glycyl-arginine-*p*-nitroanilide (Spectrozyme fXa) (K_m = 0.284 mM) (Mahdi et al., 2000). Additional experiments were performed by incubation at 142 μM TH146 or 20 μM MAP4-TH146 with 50 nM FVIIa before the addition of 70 nM sTF_{1-219}. In these experiments, hydrolysis of the substrate was measured as described above. Last, investigations determined whether TH146 and MAP4-TH146 inhibited factor IXa (FIXa). Inhibition of 3 nM FIXa was determined indirectly by measuring the activation of FX to FXa by measuring the hydrolysis of 0.4 mM *N*-(*p*-tosyl)-Gly-Pro-Arg-paranitroanilide in the presence of phospholipids vesicles and thrombin-activated factor VIIIa (5 U/ml) in 0.2 M HEPES, 0.15 NaCl, pH 7.4, supplemented with 5 mM $CaCl_2$ 0.1% polyethyleneglycol (mol. wt. 8000) and 0.2 mg/ml bovine serum albumin as reported previously (Schmaier et al.1995). In all experiments, the initial rate of hydrolysis of the substrate in the absence or presence of the peptide inhibitor was obtained over 20 min by continuous monitoring the absorbance at 405 nm and taking a reading at 2-min intervals. Equilibrium inhibition constants were calculated by determining the $K_{i,app}$ and then the K_i according to the procedure of Bieth (1984) as reported previously (Schmaier et al., 1995).

Inhibition of RPPGFK-Biotin Binding. Recombinant PAR1 exodomain ($rPAR1_{EC}$) was prepared as described previously (Hasan et al., 2003). $rPAR1_{EC}$ (1 μg/well) in 0.1 M Na_2CO_3, pH 9.6, was bound to microtiter plate wells (F96 CERT.MAXISORP, #439454; Nunc-Immuno Plate, Fisher Scientific, Chicago, IL) by incubation at 4°C overnight. After incubation, wells were washed three times with 10 mM NaH_2PO_4, 150 mM NaCl, pH 7.4, containing 0.05% Tween 20. After blocking with 1% gelatin, the bound $rPAR1_{EC}$ was incubated with 20 μM RPPGFK-biotin (Multiple Peptide Systems, Inc., San Diego, CA) in the presence or absence of various peptides 2 h at 37°C. After incubation, the wells were washed three times with 10 mM NaH_2PO_4, 150 mM NaCl, pH 7.4, containing 0.05% Tween 20 and the bound RPPGFK-biotin was detected by using Immune-Pure streptavidin horseradish peroxidase conjugate (Pierce Chemical, Rockville, IL) and peroxidase-specific fast reacting substrate turbo-3,3′5,5′-tetramethylbenzidine (turbo-TMB; Pierce Chemical) as described previously (Hasan et al., 1994). The color reaction was stopped by the addition of 1 M phosphoric acid, and the reaction was quantitated by measuring the absorbance at 450 nm in a Microplate auto reader EL311 (Bio-Tek Instruments, Winooski, VT).

Digestion of Recombinant $PAR1_{EC}$ by Proteolytic Enzymes. One microgram of recombinant exodomain of human PAR1 ($rPAR1_{EC}$) in 10 mM Tris-HCl, 200 mM NaCl, pH 8.0, was incubated at 37°C for 15 min with 0.5 μg/ml (16.7 nM) thrombocytin in the absence or presence of various concentrations of MAP4-TH146 (0.05–0.5 mM) (Niewiarowski et al., 1979; Santos et al., 2000; Hasan et al., 2003). Thrombocytin, a PAR1-activating enzyme, was a generous gift of the late Stefan Niewiarowski (Temple University, Philadelphia, PA) (Santos et al., 2000). The reaction mixture was separated on SDS-polyacrylamide gel electrophoresis and stained with R-250 Coomassie Brilliant Blue (Bio-Rad, Hercules, CA).

Ability of MAP4-TH146 to Inhibit the Enzymatic Activity of Thrombocytin. The chromogenic substrate H-D-Phe-Pip-Arg-paranitroanilide (1 mM) was incubated with thrombocytin (16.7 nM) in the absence or presence of MAP4-TH146 (0.2 mM) in 10 mM Tris-HCl, 150 mM NaCl, pH 7.6. The initial rate of hydrolysis of the substrate was determined by monitoring absorbance at 405 nm for 30 min.

Pharmacokinetic Studies. All animal studies were in accordance with the Guide for the Care and Use of Laboratory Animals. Purpose-bred beagle dogs (9–11 kg) were anesthetized with intravenous administration of sodium pentobarbital (30 mg/kg), and anesthesia was maintained by intramuscular pentobarbital (90 mg) as needed. After tracheostomy, intubation, and positive pressure ventilation with room air using a Harvard respirator (Harvard Instruments, South Natick, MA), the right jugular vein and right femoral vein were cannulated for blood collection and drug administration, respectively. Arterial blood pressure was monitored from a cannulated right carotid artery with a blood pressure transducer (Gould Inc., Cardiovascular Product, Oxford, CA). Standard limb lead II of the electrocardiogram was recorded continuously and used to monitor heart rate. After a single intravenous administration of TH146 (4.63 mg/kg in 5 ml saline infused over 1 min to each of five dogs), blood samples were collected at 1, 5, 10, 15, 20, 25, 30, 40, 60, 90, and 120 min by withdrawing 5 ml of blood into a syringe containing 3.8% sodium citrate (1:9, citrate/blood). The blood was centrifuged at 12,000*g* for 2 min at room temperature to prepare platelet-poor plasma that was stored in small aliquots at −70°C until assay. The canine plasma samples in the pharmacokinetic studies were analyzed by a hydrophobic interaction chromatographic method using a C4 column as reported previously (Hasan et al., 2001a). The pharmacokinetics was calculated using noncompartmental methods of Rowland and Tozer (1989).

Measurement of RPPGF Levels in Mouse Blood. Samples for measurement of mouse blood RPPGF were collected from untreated B6:129SF2/j mice (Jackson Laboratories, Bar Harbor, ME) or the same mice treated with 2 mg/kg RPPGF i.p. 45 min before blood draw. Mouse whole blood was drawn from anesthetized mice by venepuncture in the inferior vena cava after celiotomy into a tuberculin syringe to a total volume of precisely 0.3 ml. Immediately after blood draw, the sample was mixed with 0.9 ml of cold anhydrous ethanol to yield a final concentration of 25% in ethanol (v/v). After standing on ice for 30 to 60 min, tubes were centrifuged at 250*g* for 15 min at 4°C and the ethanolic plasma supernatant stored at −70°C until analysis.

RPPGF in the samples was analyzed by liquid chromatography-tandem mass spectrometry by the method of Murphey et al. (2001). Briefly, internal standard ([$^{13}C_2$,^{15}N-Gly^4] RPPGF) was added to ethanolic plasma supernatant, dried under nitrogen at 37°C, and extracted on a Nexus Abselut solid phase cartridge (Varian, Inc., Harbor City, CA). Gradient liquid chromatography on an Eclipse XDB-C18 column (2.1 × 50 mm, 5-μm particle; Aligent, Palo Alto, CA) was coupled to a TSQ quantum triple quadrupole mass spectrometer (Thermo Finnigan, San Jose, CA) with an electrospray source. Precursor ions for RPPGF (*m/z* 287, $[M + 2H]^{2+}$) and [$^{13}C_2$,^{15}N-Gly^4] RPPGF (*m/z* 288.5, $[M + 2H]^{2+}$) are collisionally activated at an energy of −8 eV and under 1.5 mT argon. The product ions for the transitions *m/z* 287→ *m/z* 408 and *m/z* 288.5 → *m/z* 411 were monitored for sample and standard, respectively. Quantification of RPPGF in plasma used the ratio of peak areas of product ions, *m/z* 408 to *m/z* 411. Concentrations in ethanolic supernatant were corrected for dilution by blood and reported as femtomoles per milliliter of blood (pM).

Mouse Bleeding Times. Tail bleeding times were measured by transecting the tails of anesthetized mice (50 mg/kg sodium pentobarbital) 5 mm from the tip. C57BL/6j mice from Jackson Laboratories were used for these studies. The tail was placed in 10 ml of saline at 37°C, and the time to cessation of bleeding for 20 s was determined with a stopwatch. Initial studies determined the time for maximal prolongation of the bleeding time after i.p. injection of 44 mg/kg TH146. In those investigations, tail bleeding times were performed in separate mice at 15-min intervals 15 to 120 min after i.p. injection. Subsequently, all treated mice had their bleeding times performed at 45 min.

Mouse Thrombosis Studies. Mice 6 to 16 weeks of age were anesthetized by intraperitoneal injection with sodium pentobarbital and placed in the supine position on a dissecting microscope (Nikon SMZ-2T; Mager Scientific, Inc., Dexter, MI). A midline surgical incision was made to expose the right common carotid artery and a Doppler flow probe (model 0.5 VB; Transonic Systems, Ithaca, NY) is placed under the vessel. The probe was connected to a flowmeter (Transonic model T106) and was interpreted with a computerized data acquisition program (Windaq; DATAQ Instruments, Akron, OH). Rose Bengal [4,5,6,7-tetrachloro-3′, 6-dihydroxy-2,4,5,7-tetraiodospiro (isobenzofuran-1(3*H*),9[9*H*] xanthan)-3:1 dipotassium salt; Fisher Scientific, Fair Lawn, NJ) at 50 mg/kg in 0.9% saline] was then injected into the tail vein in a 0.12-ml volume (Eitzman et al., 2000). After injection into the tail vein, a green laser light (Melles Griot, Carlsbad, CA) at a wavelength of 540 nm was applied 6 cm from the carotid artery. Flow is monitored continuously from the onset of injury. The time to occlusion was determined only after the vessel remained closed with a cessation of blood flow for 20 min.

Mouse Tail Blood Pressure Measurements. Mice were anesthetized with 40 mg/kg sodium pentobarbital by i.p. injection. After 30 min, i.p. injections of saline or drug were given, and the animals were placed into the restrainer (model #84 mouse restrainers; IITC Life Science Inc., Woodland Hills, CA) in a heating chamber (model #306 warming chamber; IITC Life Science Inc.) and kept at 28–30°C. An integrated sensor-cuff occluder (model B60-1/4; IITC Life Science Inc.) was placed around the tail and operated to stop tail pulsation on inflation and to detect the return of tail pulsations passing through the occluder cuff (Whitesall et al., 2004). The return of tail pulsations computerized blood pressure monitor and software (model 6M 229 6 channel mouse system, model 31 NIBP software; IITC Life Science Inc.) was set for three cycles per mouse and 9 s between cycles (Whitesall et al., 2004). The instrument was set for a maximum inflation pressure of 200 mm Hg. After 15 min in the chamber, the pressure cycles for each mouse were started and systolic pressure readings taken at 15, 30, 45, 60, and 75 min. Five animals (untreated or treated were examined simultaneously.

Statistical Methods. Statistical comparisons between treatment groups used the unpaired Student's *t* test or the nonparametric Mann-Whitney signed rank test as appropriate. p values <0.05 were considered significant.

Results

The angiotensin-converting enzyme breakdown product of bradykinin, RPPGF, inhibits thrombin-induced platelet aggregation and calcium mobilization and prolongs coagulant assays (Hasan et al., 1996, 2003). Previous studies prepared a combinatorial library of compounds containing natural amino acids based on RPPGF, none of which were more significantly potent (Hasan et al., 2001b). Using combinatorial libraries and empiric synthesis, a library of 72 com-

pounds consisting of D- and/or synthetic amino acids was prepared substituting various amino acids in positions one to five in RPPGF. The initial functional screening assay for all of these peptides was inhibition of γ-thrombin-induced platelet aggregation. The most potent linear peptide inhibitors of platelet aggregation when compared with RPPGF (0.68 ± 0.28 mM) are shown in Table 1. These compounds were effective at inhibiting platelet aggregation at concentrations 2.6- to 4.7-fold less than RPPGF (Table 1). The most potent overall inhibitor TH146 (rOicPGF) and its multiantigenic peptide form, MAP4-TH146, were chosen for further investigations.

In Vitro Characteristics of the RPPGF Analogs. TH146 abolished threshold γ-thrombin-induced platelet aggregation at 142 ± 20 μM, whereas its multiantigenic form, MAP4-TH146, was 7.5-fold more potent, inhibiting γ-thrombin-induced platelet aggregation at 19 ± 6 μM (Table 1). Using washed platelets, TH146 inhibited threshold α-thrombin-induced platelet aggregation 100% at 444 ± 40 μM with an IC_{50} value of 240 μM (data not shown). TH146 and MAP4-TH146 produced 50% inhibition of threshold α-thrombin-induced calcium mobilization at a concentration of about 110 and 18 μM, respectively (Fig. 1). Like inhibition of platelet aggregation, MAP4-TH146 was a more potent inhibitor than the single five-amino acid linear peptide form, TH146.

Additional studies were performed to determine whether these compounds directly interacted with thrombin similar to RPPGF (Hasan et al., 2003). There was significant prolongation ($p < 0.05$) of the APTT, PT, or TCT at 31, 62, or 7.8 μM TH146, respectively (Fig. 2A). Likewise, significant prolongation ($p < 0.05$) of the APTT, PT, or TCT occurred at 0.4, 6.25, or 1.56 μM MAP4-TH146, respectively (Fig. 2B). In these studies, the APTT and thrombin time were more sensitive to prolongation than the prothrombin time.

Because RPPGF and bradykinin interact with the active site of thrombin, investigations were performed to determine the kinetics of TH146 and MAP4TH146 inhibition of thrombin and to ascertain whether these peptides inhibit the enzymatic activity of any other coagulation enzyme(s) (Table 2) (Cleary et al., 2003; Hasan et al., 2003). TH146 and MAP4-TH146 inhibited human α-thrombin hydrolysis of Sar-Pro-Arg-pNA with a K_i value of $9.7 \pm 2.8 \times 10^{-5}$ and $4.9 \pm 1.8 \times 10^{-5}$ M, respectively (Table 2). In contrast, these peptides did not inhibit the enzymatic hydrolysis of Sar-Pro-Arg-pNA by human γ-thrombin. Furthermore, these peptides did not inhibit hydrolysis of human FXIa, FIXa, or FXa (Table 2). Alternatively, peptides TH146 and MAP4-TH146, when incubated with FVIIa before the addition of tissue factor, inhibited FVIIa with a K_i value of $4.5 \pm 0.5 \times 10^{-5}$ and $5 \pm 1.3 \times 10^{-6}$ M, respectively (Table 2). However, if there was a preformed FVIIa-TF complex, these peptides did not block the FVIIa hydrolytic activity (Table 2).

Previous investigations indicated that RPPGF also inhibited PAR1 proteolysis via two mechanisms: first by interacting with the active site of thrombin, and second by binding directly to the cleavage site of PAR1 to prevent proteolysis (Hasan et al., 2003). Investigations next determined whether these analogs of RPPGF also bound to the exodomain of human PAR1 (Fig. 3). RPPGF inhibited 20 μM RPPGF-biotin binding to $rPAR1_{EC}$ linked to microtiter plates with an IC_{50}

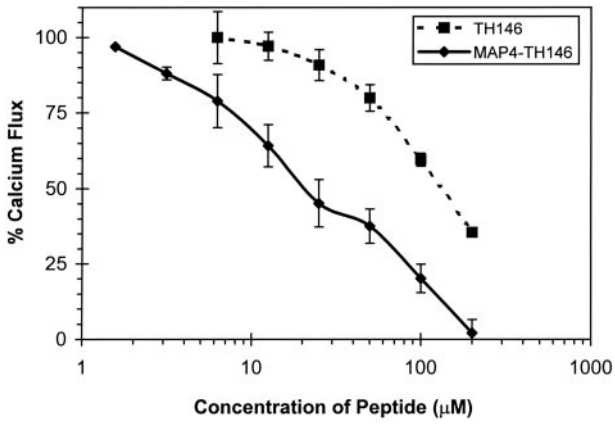

Fig. 1. Influence of TH146 and MAP4-TH146 on α-thrombin-induced intracellular calcium mobilization. Normal lung fibroblasts were loaded with Fura-2 and incubated in the absence or presence of increasing concentrations of TH146 (■) and MAP4-TH146 (♦). After incubation, cells were treated with threshold concentrations of human α-thrombin to induce maximal calcium mobilization. Values for each concentration of peptide were determined by calculating the area under the curve and are expressed as percentage of calcium flux. Samples with no peptide present were 100%. The data represent the mean ± standard deviation of at least three experiments at each concentration.

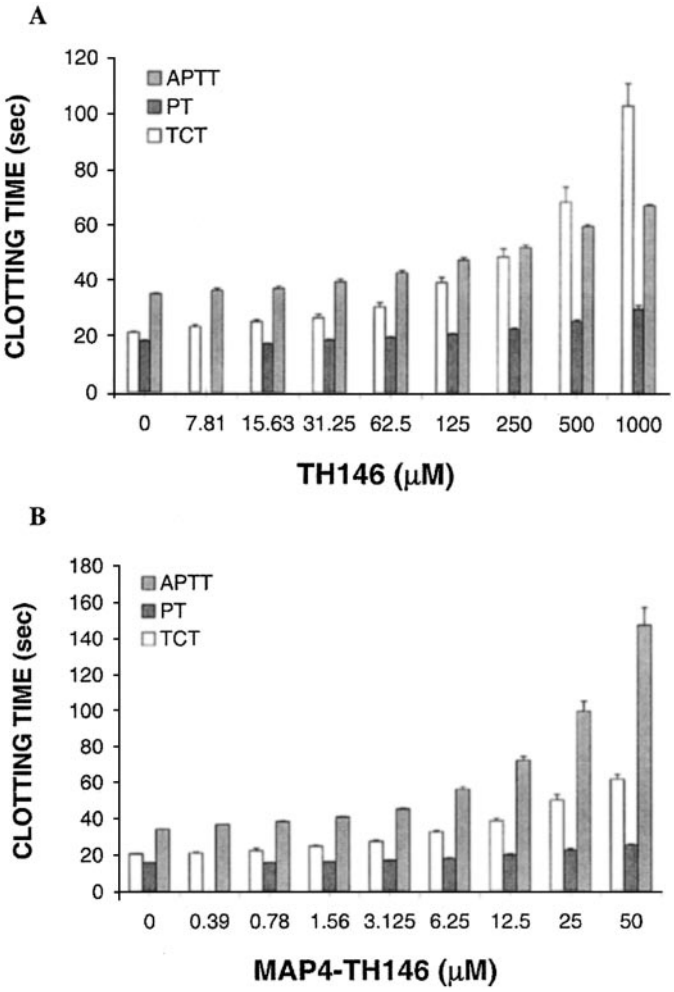

Fig. 2. Influence of TH146 and MAP4-TH146 on coagulation assays. Normal human plasma was incubated with increasing concentrations of TH146 (A) or MAP4-TH146 (B), and the APTT (gray bars), PT (dark bars), or TCT (clear bars) were determined as described under *Materials and Methods*. The data represent the mean ± standard deviation of at least three independent experiments.

TABLE 2

Direct influence of TH146 and MAP4-TH146 on the enzymatic activity of various coagulation protein enzymes

The enzymatic assays were performed as described under *Materials* and *Methods*. The data presented are the mean ± S.D. of three or more experiments. For α-thrombin (1 nM) and γ -thrombin (1 nM), the enzyme was incubated with TH146 (0.142 mM) or MAP4-TH146 (0.2 mM) for 5 min at 25°C. The reaction was initiated by the addition of the substrate Sar-Pro-Arg-pNA (0.6 mM), and the optical density was measured at 405 nm every 2 min for 20 min. FVIIa-TF samples were treated in two ways. FVIIa (50 nM) was added to 0.142 mM TH146 or 0.020 mM MAP4-TH146, followed by the addition of soluble tissue factor (70 nM), and the samples were incubated for 5 min. The reaction was initiated by the addition of the substrate methoxycarbonyl-D-cyclohexylglycyl-glycyl-arginine-*p*-nitroanilide (Spectrozyme FXa) (1.25 mM). In other experiments, a preformed complex of FVIIa (50 nM) and soluble tissue factor (70 nM) were prepared by incubation for 5 min at 25°C. The preformed FVIIa-TF complex was then mixed with each peptide and incubated for 15 min at 25°C. The reaction was initiated by the addition of the substrate Spectrozyme fXa (1.25 mM) and monitored every 2 min for 20 min.

Enzyme	TH146	MAP4-TH146
	K_i (μM) ± S.D.	
α-Thrombin	97 ± 28	49 ± 1.8
γ-Thrombin	NI	NI
Fxa	NI	NI
FIXa	NI	NI
FVIIa-TF	44.7 ± 5.4	5.0 ± 1.3
FVIIa-TF (preformed)	NI	NI
FXIa	NI	NI

NI, no inhibition.

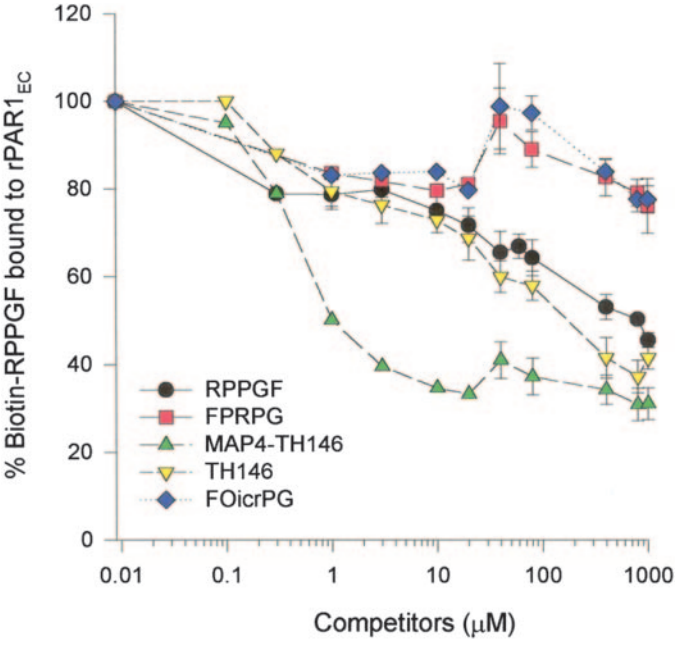

Fig. 3. Inhibition of RPPGF-biotin binding to $rPAR1_{EC}$ by RPPGF and peptide analogs. Recombinant human $PAR1_{EC}$ (1 μg/well) in 0.1 M Na_2CO_3, pH 9.6, was linked to microtiter plate wells by overnight incubation at 4°C. After washing the wells with 0.01 M sodium phosphate and 0.15 M NaCl (pH 7.4) containing 0.05% Tween and blocking with 1% gelatin, the bound protein was incubated with 20 μM RPPGFK-biotin in the absence or presence of increasing concentrations of RPPGF (●), FPRPG (■), MAP4-TH146 (▲), TH146 (▼), or FOicrPG (♦). The RPPGF-biotin bound to the cuvette well was detected streptavidin horseradish peroxidase followed by peroxidase-specific substrate and quantitated by reading absorbance at 450 nm. The data are normalized to wells containing no inhibitor that represents 100% of binding. The data are the mean ± S.D. of three experiments.

= 600 μM. Similarly, TH146 inhibited RPPGF-biotin binding with an IC_{50} = 160 μM (Fig. 3). Scrambled peptides of RPPGF (FPRPG) or TH146 (FOicrPG) did not inhibit RPPGF-biotin binding. MAP4-TH146 was the most potent inhibitor of RPPGF-biotin binding to $rPAR1_{EC}$ (IC_{50} = 1 μM). These

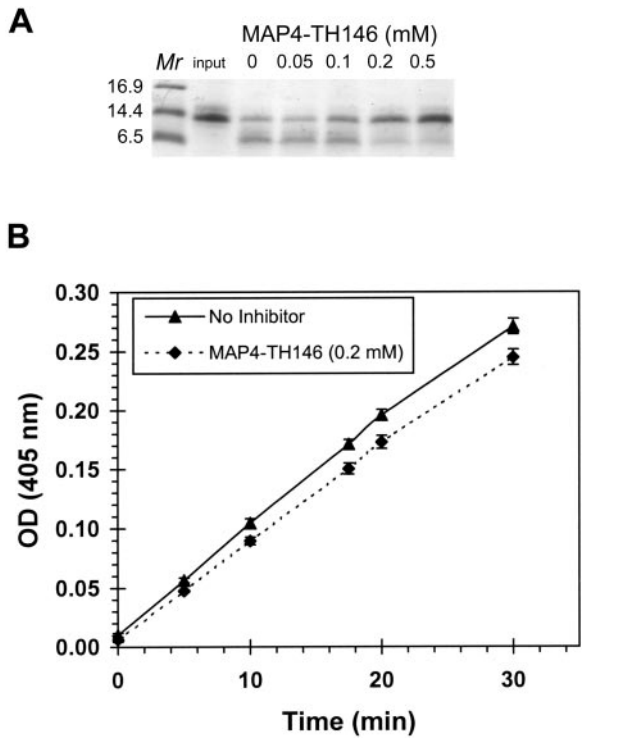

Fig. 4. MAP4-TH146 inhibits $rPAR1_{EC}$ cleavage by thrombocytin. A, $rPAR1_{EC}$ (1 μg) in 10 mM Tris-HCl, 200 mM NaCl, pH 8.0, was incubated at 37°C for 45 min with 0.5 μg/ml (16.7 nM) thrombocytin in the absence or presence of increasing concentrations of MAP4-TH146 (0.05–0.5 mM). Reaction mixtures were separated on SDS-polyacrylamide gel electrophoresis and stained with R-250 Coomassie Brilliant Blue. The lane marked "input" represents starting $rPAR1_{EC}$. B, ability of thrombocytin (16.7 nM) to hydrolyze H-D-Phe-Pip-Arg-paranitroanilide in the presence or absence of 0.2 mM MAP4-TH146. In B, the data represent the mean ± standard deviation of three replicates.

results demonstrate that, like RPPGF, these analogs also inhibited thrombin-induced platelet activation by two mechanisms, by directly interfering with the active site of thrombin and by binding to the PAR1 exodomain (Hasan et al., 2003). These features defined this class of compounds.

Because these compounds interfere with the active site of thrombin as well as bind to the exodomain of PAR1, additional experiments determined whether MAP4-TH146 blocked the proteolysis of $rPAR1_{EC}$ by thrombocytin. Thrombocytin is a snake venom enzyme that activates platelets by proteolyzing PAR1 and would not be expected to have an active site structurally like thrombin (Niewiarowski et al., 1979; Santos et al., 2000). Increasing concentrations (0.05–0.5 mM) of MAP4-TH146 prevented thrombocytin cleavage of $rPAR1_{EC}$ (Fig. 4A). Thrombocytin-induced proteolysis of $rPAR1_{EC}$ was inhibited by 0.2 mM MAP4-TH146 (Fig. 4A). When the concentration of peptide was increased to 0.5 mM, there was no significant increase in the amount of inhibition of $rPAR1_{EC}$ proteolysis. Investigations next determined whether MAP4-TH146 inhibited PAR1 proteolysis by interfering with the active site of thrombocytin. At 0.2 mM MAP4-TH146, there was little inhibition of thrombocytin hydrolysis of its chromogenic substrate. This result indicated that MAP4-TH146 had to bind to $rPAR1_{EC}$ to inhibit thrombocytin's cleavage because it did not directly inhibit the active site of thrombocytin (Fig. 4B). This fact distinguished thrombocytin from thrombin whose active site is inhibited by MAP4-

TH146. These data indicated that MAP4-TH146, like RPPGF, bound to the exodomain of PAR1 to prevent enzymatic cleavage (Hasan et al., 2003).

In Vivo Studies with RPPGF Analogs. In preparation for in vivo studies, various preliminary investigations were performed. Initially, pharmacokinetic studies were performed in dogs with TH146. After a single, 1-min intravenous infusion of TH146 at 4.63 mg/kg in 5 ml in five dogs, the $t_{1/2}\alpha$ was 3.1 ± 0.31 min (mean ± S.D.; $n = 5$ experiments) with a mean area under the curve of 171.8 ± 147 (mg/liter) min, V_d of 2650 ± 1116 ml, and clearance of 66 ± 32 ml/min/kg. These results were similar to those found with RPPGF (Hasan et al., 1999). Next, preliminary toxicology studies were performed. Mice were administered 13, 44, 131, 440 mg/kg TH146 i.p. or MAP4-TH146 at 0.20, 0.61, 2.03, 6.1, 20.3, 61, 203, and 610 mg/kg by i.p. injection to determine whether any adverse effects occurred. After i.p. injection, mice tolerated TH146 up to 440 mg/kg without observable effect. Alternatively, MAP4-TH146 was not well tolerated by mice. MAP4-TH146 at 20.3 mg/kg i.p. induced drowsiness in all mice followed by full recovery. However, ≥61 mg/kg MAP4-TH146 IP resulted in the death of all the mice treated in this manner. Furthermore, a single intravenous infusion over 5 min of MAP4-TH146 at ≥1.6 mg/kg produced transient hypotension in dogs that recovered within 30 to 60 min. Because MAP4-TH146 had these toxicities, studies with it were limited to the prevention of thrombosis (see below).

Investigations next were performed to determine whether TH146 blocked γ-thrombin-induced platelet aggregation of mouse platelets (Fig. 5). The threshold for human γ-thrombin to induce mouse platelet aggregation was 500 nM (Fig. 5). TH146 (60 μM) did not interfere with human γ-thrombin-induced mouse platelet aggregation. However 100 and 200 μM TH146 abolished γ-thrombin-induced platelet aggregation of mouse platelets. These results were unanticipated because mice only have PAR4, not PAR1 that is a target for RPPGF and its analog TH146.

Additional investigations were performed to determine whether TH146 prolonged the bleeding time in the mouse. Preliminary studies showed that after i.p. injection, the maximal prolongation of the bleeding time occurred ≥45 min. All bleeding times in treated animals were performed at 45 min after i.p. injection of the agent. Untreated mice had a tail vein bleeding time of 101 ± 9 s (mean ± S.E.M.) (Fig. 6). TH146 at 33 and 44 mg/kg i.p., prolonged the mouse tail vein bleeding time to 150 ± 11.3 s ($p < 0.23$) and 233 ± 32 s ($p < 0.003$), respectively (Fig. 6). These data suggested that TH146 influenced mouse platelet function as reflected in the bleeding time.

Investigations were next performed to determine whether RPPGF, TH146, or MAP4-TH146 prevented carotid artery thrombosis induced by photooxidation of Rose Bengal (Fig. 7). Because the genetic background of mice may influence their risk for thrombosis, the investigations were performed in two different strains of mice, B6:129SF2/j and C57BL/6j (Cui et al., 2000). In mice in a B6:129SF2/j background, RPPGF at 2 mg/kg i.p. significantly prolonged ($p < 0.0002$) the time to carotid artery thrombosis [60.4 ± 4.2 min; $n = 6$ (mean ± S.E.M.) versus 29.1 ± 2.3 min for the control; $n = 19$] (Fig. 7A). It is of interest that a 2 mg/kg i.p. injection of RPPGF did not significantly ($p < 0.4$) elevate the blood level of the peptide in mice (111 ± 35 pM control versus 106 ± 20 pM RPPGF-treated; mean ± S.E.M.; $n \geq 14$/group). RPPGF at 4 mg/kg prolonged the time to occlusion to 77 ± 3.1 min ($n = 6$) (Fig. 8A). In the C57BL/6j mice, the mean time to thrombosis in the control was 41 ± 2.4 min ($n = 11$) (Fig. 7B). RPPGF at 2 and 4 mg/kg i.p. significantly delayed ($p < 0.03$ and $p < 0.0003$, respectively) the time to thrombosis in the C57BL/6j mice to 57 ± 6.9 min ($n = 6$) and 77 ± 5.4 min ($n = 6$), respectively (Fig. 7B).

Studies next proceeded to examine whether TH146 delayed the time to thrombosis in this animal model. In mice with a B6:129SF2/j background, TH146 at 0.44 and 1.31 mg/kg significantly prolonged ($p < 0.000004$) the time to thrombosis to 49 ± 2.3 min ($n = 7$) and 63.4 ± 2.2 min ($n = 7$), respectively, compared with control animals with a mean thrombosis time of 29.1 ± 2.3 min (Fig. 7A). Similarly, in mice with the C57BL/6j background, TH146 at 4.4 mg/kg significantly delayed ($p < 0.0000005$) the time to thrombosis to 71 ± 2.5 min ($n = 6$) compared with control animals with a mean thrombosis time of 41.1 ± 2.4 min (Fig. 7B). In B6:129SF2/j mice, TH146 was a 3- to 5-fold more potent inhibitor than wild-type peptide RPPGF. In C57BL/6j mice,

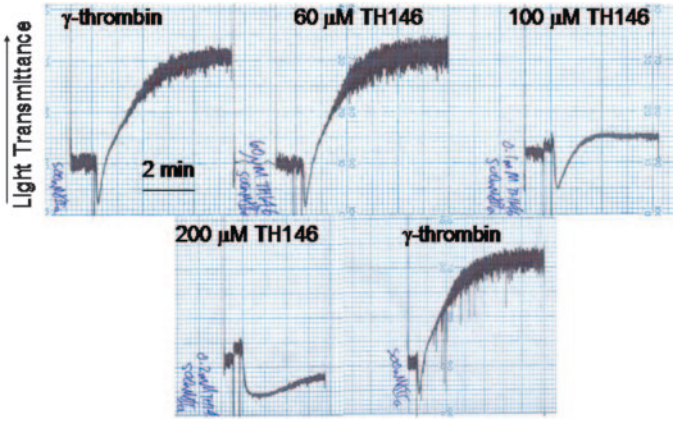

Fig. 5. TH146 inhibits thrombin-induced mouse platelet aggregation. PRP from 10 mice were pooled, the platelet count was adjusted to 2.5 × 10^8/ml, and the threshold for human γ-thrombin-induced platelet aggregation (500 nM) was obtained. The influence of 60 to 200 μM TH146 on human γ-thrombin-induced mouse platelet aggregation was determined. This figure is a representative experiment of three experiments. The panels shown are one continuous experiment from left to right and top to bottom.

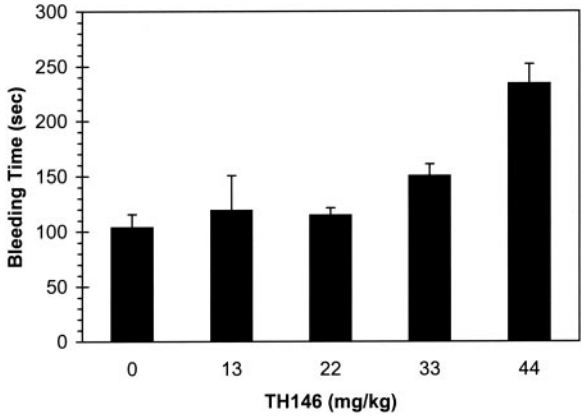

Fig. 6. Prolongation of mouse bleeding times. C57BL/6j mice were given injections of TH146 (13–44 mg/kg) i.p. Forty-five minutes after injection, the mouse tail bleeding time was determined. These data are the mean ± S.D. of five or more experiments at each concentration of the inhibitor.

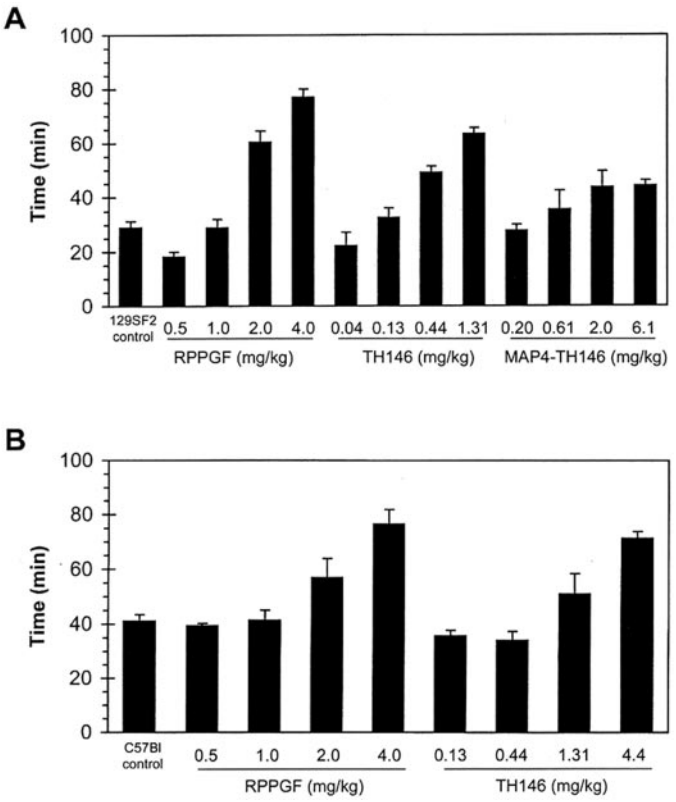

Fig. 7. Influence of RPPGF and analogs on mouse carotid artery thrombosis. B6:129SF2/j (129SF2) mice (A) or C57BL/6j (C57Bl) mice (B) were prepared for study for the time to carotid artery thrombosis initiated by photooxidation of Rose Bengal in the absence or presence of 0.5 to 4.0 mg/kg RPPGF, 0.04 to 4.4 mg/kg TH146, or 0.2 to 6.1 mg/kg MAP4-TH146 after i.p. injection. The time to carotid artery was measured in at least five animals in each group. The data are expressed as mean ± S.D.

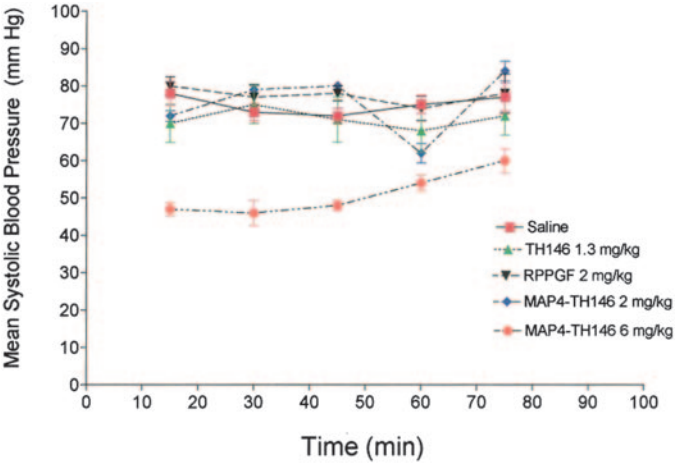

Fig. 8. Influence of RPPGF and analogs on mouse blood pressure. C57Bl mice were treated with sodium pentobarbital and after 30 min given saline, 1.3 mg/kg TH146, 2 mg/kg RPPGF, 2 mg/kg MAP4-TH146, or 6 mg/kg MAP4-TH146 by i.p. injection. The mean blood pressure was measured in the treated animals 15 min after i.p. injection at 15-min intervals for 75 min (see *Materials and Methods*). The values shown are the mean ± S.E.M. of six or more experiments.

there were no differences in efficacy. Moreover, mice in B6:129SF2/j backgrounds were more sensitive to RPPGF or TH146 to delay thrombosis than animals in C57BL/6j backgrounds.

Further studies were performed with MAP4-TH146. Although a much more effective inhibitor of in vitro platelet aggregation than TH146, MAP4-TH146 at 2 and 6.1 mg/kg i.p. inhibited thrombosis less in B6:129SF2/j mice (Fig. 7A). At 2 and 6.1 mg/kg MAP4-TH146 i.p., the delay in time to thrombosis was significant compared with control ($p < 0.03$), but only to 43.7 ± 6 min ($n = 6$) and 44.2 ± 2.1 min ($n = 5$), respectively. In mice treated with 6.1 mg/kg MAP4-TH146, swelling of all the tissues was noted in the surgical field where the right carotid artery was exposed. These data suggested that the multiantigenic peptide had additional in vivo effects that interfered with its ability to prevent thrombosis not observed with the linear peptide. Last, it was observed that the bradykinin B2 receptor antagonist HOE140, which is structurally similar to TH146, also delayed the time to thrombosis in B6:129SF2/j mice when given at i.p. at 2.7 and 9.1 mg/kg to 44.7 ± 3.2 min ($n = 3$) and 73.3 ± 5.1 min ($n = 4$), respectively (data not shown).

Because there was no increased protection from vessel occlusion at higher doses of MAP4-TH146 and these animals had obvious tissue swelling when treated with ≥6.1 mg/kg MAP4-TH146, the animals had their blood pressure measured under conditions that simulated the thrombosis model. In general, mice that were treated with sodium pentobarbital had a drop in their mean blood pressure from 120 mm Hg to ~70 to 80 mm Hg (data not shown). Animals that were treated with TH146 at 1.3 mg/kg i.p. and RPPGF at 2 mg/kg did not have a significant change ($p > 0.05$) in the mean blood pressure from those animals treated with saline (Fig. 8). Animals treated with 2 mg/kg i.p. MAP4-TH146 did not have a significant drop ($p < 0.04$) in their mean blood pressure at 15 to 60 min. All animals that were treated with MAP4-TH146 at 6 mg/kg i.p. did have a significant drop ($p < 0.001$) in their mean blood pressure to 40 to 50 mm Hg at all times during the experiment. These results are consistent with the blood pressure lowering effect previously reported for MAP4-RPPGF and may account for the reduced thrombosis protection and tissue swelling seen with higher concentrations of MAP4-TH146 (Hasan et al., 2001a).

Discussion

These investigations indicate that RPPGF and structural analogs consisting of D- and synthetic amino acids interfere with thrombin's activities in vitro and can prolong bleeding times and delay the time to thrombosis in vivo. The basis for the design of these present compounds was the observation that the bradykinin B2 receptor antagonist HOE140 delays the time to thrombosis in mice. These data indicate that HOE140 has a direct antithrombin effect or that inhibition of the bradykinin B2 receptor activation influences the risk to thrombosis in the intravascular compartment. Three- to 12-fold more potent RPPGF-like compounds were prepared using D- and synthetic amino acid substitutions (Stewart et al., 1999, 2001).

The compounds TH146 and MAP4-TH146 seem to have the same mechanism(s) of action as RPPGF (Hasan et al., 2003). Both compounds block soluble biotinylated RPPGF from binding the recombinant exodomain of human PAR1 (Hasan et al., 2003). The fact that MAP4-TH146 blocks thrombocytin proteolysis of the recombinant exodomain of human PAR1 indicates that it must be binding to PAR1 to prevent cleavage because it does not inhibit the enzymatic activity of throm-

bocytin to hydrolyze its chromogenic substrate. Furthermore, both compounds also interact directly with thrombin because they prolong various plasma coagulation assays mediated by thrombin formation (Hasan et al., 2003). Like previous studies with MAP4-RPPGF, both TH146 and MAP4-TH146 have a greater degree of prolongation of the APTT over the PT (Hasan et al., 2001a). Previous studies have suggested that this dichotomy of results could be due to MAP4-RPPGF interfering with thrombin activation of factor XI (Hasan et al., 2001a). It was unexpected to learn that TH146 and MAP4-TH146 also inhibit factor VIIa without blocking the preformed FVIIa-TF complex. This activity must additionally contribute to their antithrombotic effect in vivo, but it would not account for the greater prolongation of the APTT over the PT.

In vivo studies show that TH146 has a similarly delayed clearance after intravenous infusion as has been noted for RPPGF (Hasan et al., 1999; Murphey et al., 2000). The toxicology studies showed that MAP4-TH146 was much less tolerated than TH146. MAP4-TH146 injection results in tissue edema, hypotension, and death at concentrations near the dose necessary to delay thrombosis formation. These complications are not seen with TH146. Previous studies showed that MAP4-RPPGF induces hypotension upon a single, intravenous infusion (Hasan et al., 2001a). This hypotension was blocked by pretreating the animal with the bradykinin B2 receptor antagonist HOE140. Hypotension and tissue edema seen with MAP4-TH146 infusion are consistent with stimulation of the bradykinin B2 receptor. RPPGF has been demonstrated not to bind to the bradykinin B2 receptor and does not produce vasodilation or stimulate tissue-type plasminogen activator release, two well characterized bradykinin B2 receptor responses, in the human vasculature (Malave et al., 2003). However, it is possible that a cluster peptide of closely associated RPPGF or TH146 molecules could stimulate this receptor to give the deleterious effects observed.

The finding that TH146 inhibits thrombin-activation of mouse platelets was not expected. Mice do not have PAR1 on their platelets; they have PAR3 and PAR4. It is not possible that the amount of TH146 used to inhibit human γ-thrombin-induced platelet aggregation ex vivo was at a concentration sufficient to directly block the enzymatic activity of the thrombin. Although TH146 could interact with the active site amino acids of γ-thrombin, our studies show that TH146 does not inhibit the hydrolytic activity of γ-thrombin on a small molecule substrate (Ayala et al., 2001; Cleary et al., 2002). This assessment indicates that the prolongation of the mouse bleeding time and delay in thrombosis after free radical-induced vessel injury cannot be explained by direct inhibition of endogenous thrombin. The amount of TH146 administered to the animal IP and entering the intravascular compartment also must be below the amount necessary to directly block endogenous mouse thrombin. These in vivo studies suggest that TH146 may also be interacting with mouse PAR4. Recent preliminary data from our laboratory indicate that RPPGF and TH146 directly bind to a recombinant exodomain of human PAR4 (Schmaier et al., 2003). Thus, RPPGF and its analogs seem to interact with the exodomains of both human PAR1 and PAR4 (Hasan et al., 2003; Schmaier et al., 2003).

Although it is not yet known whether RPPGF in vivo ever achieves a sufficiently high concentration to function as an antithrombin, it was surprising to us that after a 2 mg/kg i.p. injection of RPPGF, the picomolar blood levels of the RPPGF were not significantly elevated in the treated mice. These data suggest that the peptide is binding to different sites and is not available to circulate in the intravascular compartment. Previous in vitro studies showed that when RPPGF was added to a suspension of PRP, 97% of the peptide bound to the platelet pellet (Hasan et al., 1999). These results also suggest that small changes in the intravascular concentration of RPPGF may influence the anticoagulant state of an animal.

Further analogs of TH146 have the potential to be a novel antiplatelet agent. It is of interest that its effective antithrombotic dose of 0.44 mg/kg i.p. in the B6:129SF2/j mice is less than that required for in vivo efficacy of two small molecule, nonpeptide mimetics that have been published recently (Derian et al., 2003; Kato et al., 2003). Moreover, TH146 at 3 orders of magnitude higher concentration had no adverse effect on mice. Unlike the small nonpeptide mimetic compounds that are directed only to the PAR1 signaling site, TH146 and related compounds interfere with both PAR1 and PAR4 activation as well as have some inhibitory effect directly on thrombin and factor VIIa. These combined inhibitory effects must summate in vivo to contribute to the antithrombotic effect in the whole animal. These findings suggest that RPPGF and related compounds are novel antagonists to thrombin, factor VIIa, and thrombin activation of platelets, being a single class of compounds that interact with both thrombin receptors on human platelets. These investigations indicate that prevention of thrombin cleavage of PAR1 and 4 also is an appropriate target to develop antithrombin, antiplatelet agents.

Acknowledgments

We thank Dr. John Stewart (University of Colorado School of Medicine, Denver CO) for helpful discussions in the design of these compounds. We also appreciate the assistance of Dr. Ziaeddin Shariat-Madar (University of Michigan) with the pharmacokinetic calculations.

References

Ayala YM, Cantwell AM, Rose T, Bush LA, Arosio D, and DiCera E (2001) Molecular mapping of thrombin-receptor interactions. *Proteins* **45:**107–116.

Bieth JG (1984) In vivo significance of kinetic constants of protein proteinase inhibitors. *Biochem Med* **222:**209–223.

Cleary DB, Ehringer WD, and Maurer MC (2003) Establishing the inhibitory effects of bradykinin on thrombin. *Arch Biochem Biophys* **410:**96–106.

Cleary DB, Trumbo TA, and Maurer MC (2002) Protease-activated receptor 4-like peptides bind to thrombin through an optimized interaction with the enzyme active site surface. *Arch Biochem Biophys* **403:**179–188.

Cook JJ, Sitko GR, Bednar B, Condra C, Mellott MJ, Feng DM, Nutt RF, Shafer JA, Gould RJ, and Connolly TM (1995) Molecular and cellular cardiology: an antibody against the exosite of the cloned thrombin receptor inhibits experimental arterial thrombosis in the African green monkey. *Circulation* **91:**2961–2971.

Cui J, Eitzman DT, Westrick RJ, Christie PD, Xu ZJ, Yang AY, Purkayastha AA, Yang TL, Metz AL, Gallagher KP, et al. (2000) Spontaneous thrombosis in mice carrying the factor V Leiden mutation. *Blood* **96:**4222–4226.

Derian CK, Damiano BP, Addo MF, Darrow AL, D'Andrea MR, Nedelman M, Zhang HC, Maryanoff BE, and Andrade-Gordon P (2003) Blockage of the thrombin receptor protease-activated receptor-1 with a small-molecule antagonist prevents thrombus formation and vascular occlusion in nonhuman primates. *J Pharmacol Exp Ther* **304:**855–861.

Eitzman DT, Westrick RJ, Nabel EG, and Ginsburg D (2000) Plasminogen activator inhibitor-1 and vitronectin promote vascular thrombosis in mice. *Blood* **95:**577–580.

Fisher SK, Domask LM, and Roland RM (1989) Muscarinic receptor regulation of cytoplasmic Ca^{2+} concentrations in human SK-N-SH neuroblastoma cells: Ca^{2+} requirements for phospholipase C activation. *Mol Pharmacol* **35:**195–204.

Hanson SR and Harker LA (1988) Interruption of acute platelet-dependent thrombosis by the synthetic antithrombin D-phenylalanyl-L-prolyl-L-arginyl chloromethyl ketone. *Proc Natl Acad Sci USA* **85:**3184–3188.

Hasan AAK, Amenta S, and Schmaier AH (1996) Bradykinin and its metabolite, Arg-Pro-Pro-Gly-Phe, are selective inhibitors of α-thrombin-induced platelet activation. *Circulation* **94:**517–528.

Hasan AAK, Cines DB, Zhang J, and Schmaier AH (1994) The carboxyl terminus of bradykinin and amino terminus of the light chain of kininogens comprise an endothelial cell binding domain. *J Biol Chem* **269:**31822–31830.

Hasan AAK, Rebello SS, Smith E, Srikanth S, Werns S, Driscoll E, Faul J, Brenner D, Normolle D, Lucchesi BR, et al. (1999) Thrombostatin inhibits induced canine coronary thrombosis. *Thromb Haemostasis* **82:**1182–1187.

Hasan AAK, Schmaier AH, Warnock M, Normolle D, Driscoll E, Lucchesi BR, and Werns SW (2001a) Thrombostatin inhibits cyclic flow variations in stenosed canine coronary arteries. *Thromb Haemostasis* **86:**1296–1304.

Hasan AAK, Warnock M, Nieman M, Srikanth S, Mahdi F, Krishnan R, Tulinsky A, and Schmaier AH (2003) Mechanisms of Arg-Pro-Pro-Gly-Phe inhibition of thrombin. *Am J Physiol* **285:**H183–H193.

Hasan AAK, Warnock M, Srikanth S, and Schmaier AH (2001b) Developing peptide inhibitors to thrombin activation of platelets from bradykinin analogs. *Thromb Res* **104:**451–465.

Kato Y, Kita Y, Hirasawa-Taniyama Y, Nishio M, Mihara K, Ito K, Yamanaka T, Seki J, Miyata S, and Mutoh S (2003) Inhibition of arterial thrombosis by a protease-activated receptor 1 antagonist, FR171113, in the guinea pig. *Eur J Pharmacol* **473:**163–169.

Mahdi F, Rehemtulla A, Van Nostrand WE, Bajaj SP, and Schmaier AH (2000) Protease nexin-2/amyloid β-protein precursor regulates factor VIIa and factor VIIa-tissue factor complex. *Thromb Res* **99:**267–276.

Malave HA, Murphey LJ, Vaughan DE, Biaggioni I, and Brown NJ (2003) RPPGF inhibits alpha-thrombin and gamma-thrombin-induced platelet aggregation in the human vasculature. *Arterioscler Thromb Vasc Biol* **23:**P106.

Meloni FJ and Schmaier AH (1991) Low molecular weight kininogen binds to platelets to modulate thrombin-induced platelet activation. *J Biol Chem* **266:** 6786–6794.

Murphey LJ, Hachey DL, Oates JA, Morrow JD, and Brown NJ (2000) Metabolism of bradykinin in vivo in humans: identification of BK1–5 as a stable plasma peptide metabolite. *J Pharmacol Exp Ther* **294:**263–269.

Murphey LJ, Hachey DL, Vaughan DE, Brown NJ, and Morrow JD (2001) Quantification of BK1–5, the stable bradykinin plasma metabolite in humans, by a highly accurate liquid-chromatographic tandem mass spectrometric assay. *Anal Biochem* **292:**87–93.

Niewiarowski S, Kirby EP, Brudzynski TM, and Stocker K (1979) Thrombocytin, a serine protease from Bothrops atrox venom. 2. Interaction with platelets and plasma-clotting factors. *Biochemistry* **18:**3570–3577.

Prieto AR, Ma H, Huang R, Khan G, Schwartz KA, Hage-Korban EF, Schmaier AH, Davis JM, Hasan AAK, and Abela GS (2002) Thrombostatin, a bradykinin metabolite, reduces platelet activation in a model of arterial wall injury. *Cardiovas Res* **53:**984–992.

Puri R, Zhou F, Hu CJ, Colman RF, and Colman RW (1991) High molecular weight kininogen inhibits thrombin-induced platelet aggregation and cleavage of aggregin by inhibiting binding of thrombin to platelets. *Blood* **77:**500–507.

Rowland M and Tozer T (1989) *Clinical Pharmacokinetics: Concepts and Application*, 2nd ed, Lea & Febiger, Philadelphia.

Santos BF, Serrano SM, Kuliopulos A, and Niewiarowski S (2000) Interaction of viper venom serine peptidases with thrombin receptors on human platelets. *FEBS Lett* **477:**199–202.

Schmaier AH, Dahl LD, Hasan AAK, Cines DB, Bauer KA, and Van Nostrand WE (1995) Factor IXa inhibition by protease nexin-2/amyloid β-protein precursor on phospholipid vesicles and cell membranes. *Biochemistry* **34:**1171–1178.

Schmaier AH, Pagan-Ramos E, Warnock M, Krijanovski Y, Hasan AAK, and Nieman MT (2003) Arg-Pro-Pro-Gly-Phe binds to the exodomain of human protease activated receptor 4 (PAR4) to prevent thrombin proteolysis and platelet activation (Abstract). *Blood* **102 (Suppl 1):**776a–777a.

Stewart JM, Gera L, York EJ, Chan DC, and Bunn P (1999) Bradykinin antagonists: present progress and future prospects. *Immunopharmacology* **43:**155–161.

Stewart JM, Gera L, York EJ, Chan DC, Whalley EJ, Bunn PA Jr, and Vavrek RJ (2001) Metabolism-resistant bradykinin antagonists: development and applications. *Biol Chem* **382:**37–41.

Weiss EJ, Hamilton JR, Lease KE, and Coughlin SR (2002) Protection against thrombosis in mice lacking PAR3. *Blood* **100:**3240–3244.

Whitesall SE, Hoff JB, Vollmer AP, and D'Alecy LG (2004) Comparison of simultaneous measurement of mouse systolic arterial blood pressure by radiotelemetry and tail-cuff methods. *Am J Physiol* **286:**H2408–H2415.

Address correspondence to: Dr. Alvin H. Schmaier, University of Michigan, Division of Hematology and Oncology, 5301 MSRB III, 1150 West Medical Center Dr., Ann Arbor, MI 48109-0640. E-mail: aschmaie@umich.edu